NON-LOADBEARING LIGHT STEEL FRAMING WALLS UNDER FIRE

Seddik M. Khetata [*]
PhD Student
USAL
Spain

Paulo A. G. Piloto
Professor
IPB
Bragança, Portugal

Ana B. R. Gavilán
Professor
USAL
Spain

Keywords: Fire tests; LSF walls; Numerical Simulation; Fire Resistance.

1. INTRODUCTION

The light steel frame (LSF) construction technology started to be widely used in different types of buildings, replacing the traditional construction methods due to its light weight characteristics. Steel is recycled, dimensional stable, and ease of installation. LSF and prefabricated panels are widely used in non-loadbearing walls. The LSF walls are usually made with studs and tracks that require fire protection, normally achieved by a single plasterboard, by composite plates, or by insulation of the cavity. The partition walls are fire rated for the integrity (E) and insulation (I). The insulation capacity (I) is the ability of the element of construction to withstand fire exposure by one side, without the transmission of significant heat to the unexposed side. Six fire tests were developed to define the fire resistance according to EN1363-1 [1] and EN1364-1 [2], with the main objective to evaluate the influence of the protection layers and the influence of the cavity insulation material. Numerical models are also validated with experimental tests.

Different studies and investigations were developed with the aim of testing the influence of using different configurations of LSF walls, different protection materials such as plasterboards and insulation materials. One of the first research in this domain was developed in the Cornell University in 1963 by G. Winter, which did serval analyses on the effects of cold-straining on structural sheet steels, including the corner properties of cold-formed steel shapes, the effects of cold-forming on the mechanical properties and on structural behaviour of members [3]. In 1973, B. C. Son and H. Shoub developed two fire-endurance tests on double-wall assemblies. They

[*]Corresponding author – University of Salamanca. Patio de Escuelas, 1, 37008, Salamanca, Spain.
Telef.: +351 936 995066, E-mail: khetatamohamedseddik@gmail.com

concluded that the temperature data for the second test also indicates a much slower temperature rise in the fire-exposed gypsum board and a better solution on practice would be the use of a two-layer construction plates with staggered application of board joints to eliminate direct heat access to the steel studs in joints [4]. Kenneth J. Schwartz and T. T. Lie in 1985 [5], studied the effect of the heat transmission to prevent ignition of the materials in contact with the unexposed side of the partition wall. Authors analysed data from previous experimental tests and made more experiments to evaluate the insulation criteria of the standard ASTM E119. The information helped to understand the relationship between the unexposed surface temperature rise criteria and the ignition temperature of common combustible materials. The Australian standard was submitted to a major revision in 1988, following the specification of AISI in 1980 and 1986 [6]. The AISI produced a new limit version on its 1986 version in 1991, called the load and resistance factor design specification (LRFD). In the year 1990, the Australian standard AS4100 published the limit stat design criterion based on the approach of LRFD. In 1993, the Australian and New Zealand standards present a limit state design for cold formed steel structures in both countries. In 1998 the British Standard Institute published the part 5 on NS5950 to guide the design of cold formed steel structures for the ultimate limit state. Other international standards for cold formed structural steel, such as Eurocode 3, are already with the limit state format [6]. In 1995 J. T. Hans Gerlich presented a report developing the knowledge about the performance of loadbearing light steel frame (LSF) drywall systems and to model the performance against the IS0834 time-temperature curve and real compartment fires [7]. In 2000 Alfawakhiri and Sultan presented a comparison between experimental tests and numerical simulation, demonstrating how different heating regimes applied in cold formed steel studs cause different structural failure modes [8]. An experimental investigation was also developed by Ghazi Wakili and E. Hugi in 2009, dealing with thermal properties of the materials and comparing the fire behaviour of four types of gypsum, investigating also the temperature history evolution comparison for a box protected steel column, finding more than 100 º C of maximum difference on the steel temperature after 90 minutes of fire exposure, when considering different these types of gypsum materials [9]. In 2014 Nassif et al. published results of serval full scale fire tests on the steel-stud gypsum-faced partition wall. The tests results were used to verify a proposed numerical procedure to be used in predicting the thermo-mechanical behaviour. The measured temperatures across the wall agreed with the predicted values until the falling off of the gypsum board [10]. Jonathan Vallée in 2016 did numerical validations, using ABAQUS and FDS to simulate furnace tests developed for LSF partition walls, testing empty cavities and insulated cavities. Author concluded that insulation material in the cavity can improve the fire resistance, when considering the insulation criterion, especially when ablation of the gypsum plates occurs [11].

The fire performance on LSF walls started to be investigated in 2017 at the Polytechnic Institute of Bragança (IPB) with the aim of: 1- developing accurate numerical models based on the thermal analysis with fluid structure interaction, [12]; 2- validate the numerical models with experimental tests developed by others, [13]; 3- analysing the fire performance of LSF using the simplified one dimensional heat flow, [14]; 4- presenting a sequential numerical model to study the fire resistance of LSF walls made with composite panels under loadbearing conditions in 2018 [15] and; and 5- predict the load effect on the LSF walls under fire conditions using numerical simulations [16]. The fire tests were simulated in 2019 using a hybrid 3D finite element model. The results agree well with the experimental tests, which allows to develop future parametric analysis [17]. Dias, Keerthan, and Mahendran in 2019 presented the results of 13 small-scale fire tests conducted on

non-load bearing steel and gypsum plasterboard sheathed panels and walls and numerical simulations were conducted to evaluate the enthalpies of plasterboards and steel sheathing. They concluded that retention of vaporised water from the calcination process within the plasterboard due to the confinement provided by steel sheathing is a crucial factor that improves the fire performance of such walls [18].

This investigation is related with the fire resistance for insulation of non-load bearing walls made with LSF protected with composite plates. Two different LSF are compared (3 and 5 studs) along with two insulation materials for the cavity (rock wool and ceramic fibre) and different combination materials for the composite plate (gypsum, cork, wood).

2. FIRE TESTS

2.1 Conditions and criteria

Six small-scale LSF walls were tested in a small fire resistance furnace. This furnace is able to follow the standard fire ISO834 (International Organization for Standardization, 1999) [19], see Eq. 1. The generic standard EN 1363-1 [1] and the specific standard EN1364-1 [2] were used to define the fire resistance (I) of the six non-load bearing walls. The fire resistance (I) is the ability of the element to withstand exposure to fire only on one side, without significant heat transfer from the exposed side to the unexposed side. The heat transfer should be limited to avoid that the unexposed surface or any material close to that surface is ignited. The fire rating (I) of a partition wall should be defined based on the shortest time for which the criteria of maximum or the average temperature increase are satisfied in any discrete area. The fire performance level used to define the insulation (I) shall be calculated on the basis of the increase in the average temperature on the unexposed side, limited to 140 ° C above the initial average temperature, or, based on the increase of the maximum temperature in any location, limited to 180 ° C above the initial average temperature.

$$\theta_{\mathrm{q}} = 20 + 345 \log 10(8t + 1) \quad (1)$$

2.2 Wall specimens

The fire tests were developed in the furnace at the IPB, see figure1. Different wall configurations were tested (number of studs and the spacing in between) (see table 1), the protection layers and the insulation material included in the cavity. These LSF walls are made with cold formed steel profiles, using stud profiles C90x43x15x1.5, for the 3-stud configuration (10, 11, 12 and 15) and for the 5-stud configuration (13, 14). All studs were fixed with 2 track profiles U93x43x1.5 (see Figure 1) from the top and from the bottom of the wall, using self-drilling screw with a diameter of 4.2 mm and length of 19 mm, positioned at geometry centre of each joint along their perimeter (position 0) in figure 2, forming a cavity thickness of 90 mm. All profiles have the steel grade S280GD. The steel structure was fixed to the 3 edges of the furnace frame (left side, bottom and top) allowing a free edge, properly filled with ceramic fibre on the right side (gap size equal to 25

mm). All the wall borders were filled with gypsum as shown in Figure 1. Due to the dimensions of the furnace, the specimens were modified to fit the furnace frame, which do not present the real dimensions required by the standard EN 1364-1 [2] in fire tests. All the other condition specified in this standard were met, as well as all the general requirements for standard fire tests EN1363-1 [1].

Table 1: LSF wall specimens: Materials and geometry.

Specimen ID	LSF studs	**Spacing** mm	Cavity kg/m^3	Layer 1 mm	Layer 2 mm	Layer 3 mm
10	3	466	Rockwool/75	12.5 Gypsum	-	-
11	3	466		12.5 Gypsum	-	12.5 Gypsum
12	3	466		12.5 Gypsum	10 Cork	12.5 Gypsum
13	5	233		12.5 Gypsum	10 Cork	12.5 Gypsum
14	5	233		10 (OSB)	12.5 Gypsum	12.5 Gypsum
15	3	466	Superwool/128	12.5 Gypsum	-	-

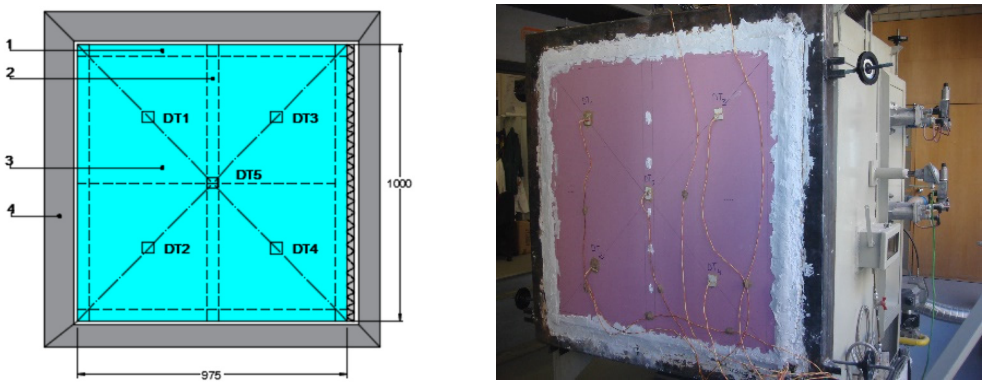

Figure 1: LSF wall specimens (dimensions in mm): tracks (1), studs (2), layer plates (3), furnace frame (4). Positions for the disc thermocouples (DTi) in the unexposed surface.

The different steps to fix the protection layers into the steel structure from both sides (exposed and unexposed) were done using different self-drilling screws. The wall specimens 10 and 15 were made with 3 studs and one gypsum board fixed by 5 self-drilling screws with a diameter of 4.8 mm and length of 32 mm in each stud spaced every 152 mm (vertical direction), see screw position 1 see Figure 2. Four screws were included in the horizontal direction. For the other tests, the same self-drilling screws were used to fix the first plasterboard (position 1) and additional self-drilling screws with a diameter of 4.8 mm and length of 50 mm were used to fix the second gypsum layer (position 2). Self-drilling screws with 63 mm of length and 5.5 mm of diameter were used to fix the third layer in tests 12, 13 and 14, (position 3), in addition to the others self-drilling screws used to fix layers 1 and 2, all spaced every 91 mm in vertical direction. More details about the distribution of the screws along the steel structure (studs and tracks) to fix the plasterboards and the number of protection layers are presented in Figure 2.

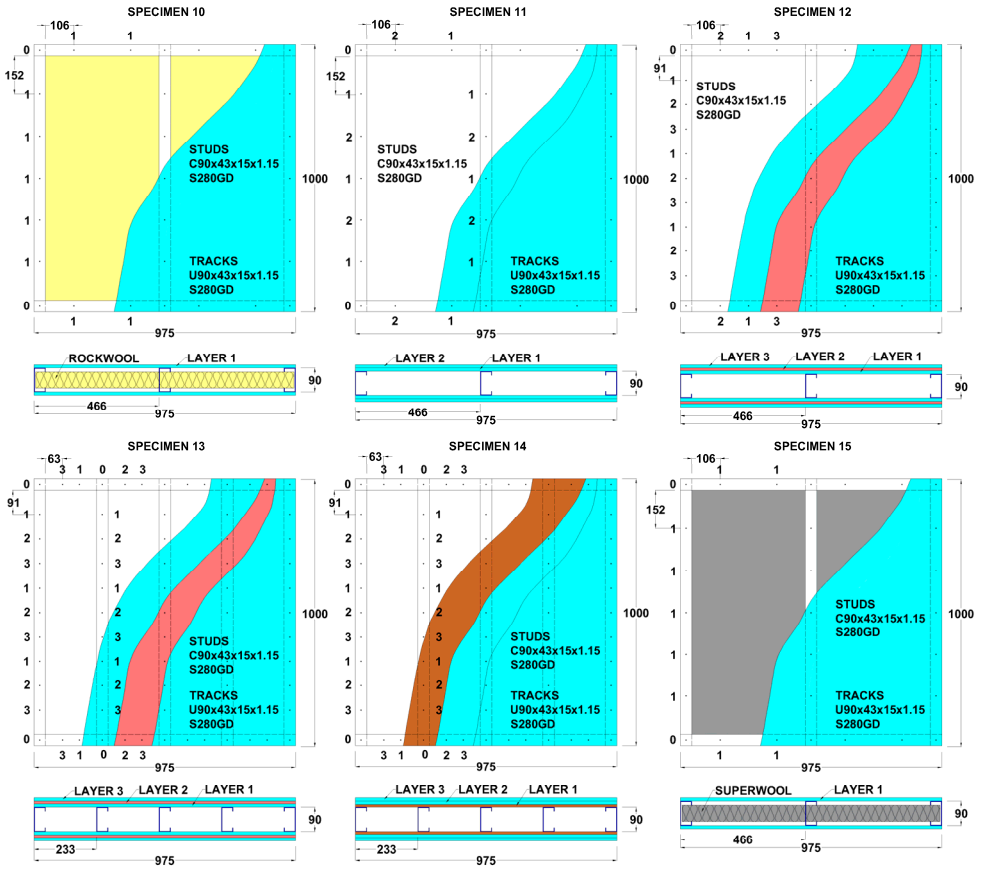

Figure 2: Assembly of the LSF wall specimens (dimensions in mm).

2.3 Instrumentation

The data acquisition system MGCPlus (HBM) was used to collect the temperature values, using a frequency of acquisition of 1 Hz. A total of 22 channels were available for the measurements. Additionally, an IR thermal camera, with the resolution of 320x240 pixels, was used to register the unexposed temperature field, FLIR BT Series T365. The frequency of acquisition of the camera was set to 1.25 Hz, with a scale temperature between 15 ° C and 250 ° C. Serval K type thermocouples with diameter of 0.7 mm were attached into the specimen with different formats for temperature measurement: copper disk with plasterboard protection (DTi) for measuring the unexposed surface temperature; plate thermocouples (PTi) were fixed at the mid height of the cavity to determine the average temperature (CAV) defined by the studs and tracks and also the ambient temperature (located 200 mm away from the unexposed surface); the hot joint made with twisted thermocouples cables (WTi) were used to measure the temperature in between plates and inside the insulation material applied in cavity; welded hot joint applied on cold formed steel

profiles (WTi) were used for measuring the temperature of the steel profiles in three different regions (hot flange-HF, web- WEB and cold flange – CF); sheath thermocouples (BTi) were used for measuring the temperature on the exposed surface. The number of thermocouples depends on the configuration of the wall specimen, see Figure 3.

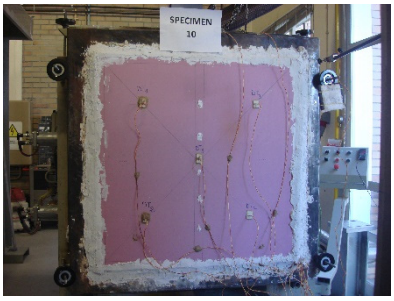

a) Initial state of wall specimen 10.

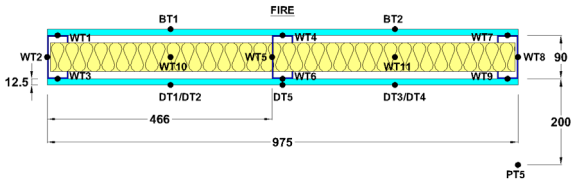

b) Thermocouples position in specimen 10.

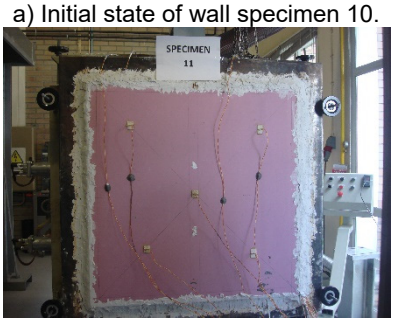

c) Initial state of wall specimen 11.

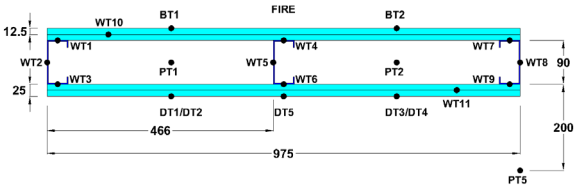

d) Thermocouples position in specimen 11.

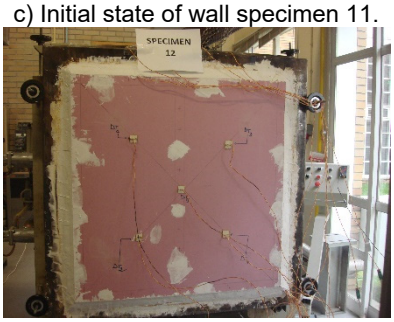

e) Initial state of wall specimen 12.

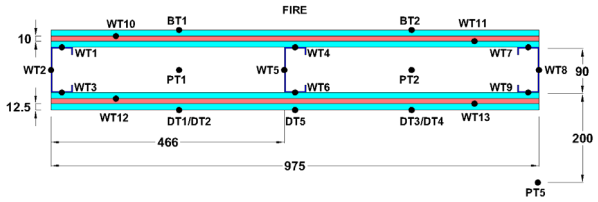

f) Thermocouples position in specimen 12.

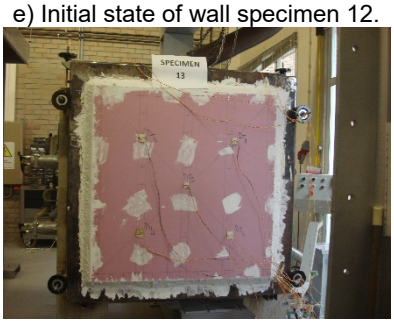

g) Initial state of wall specimen 13.

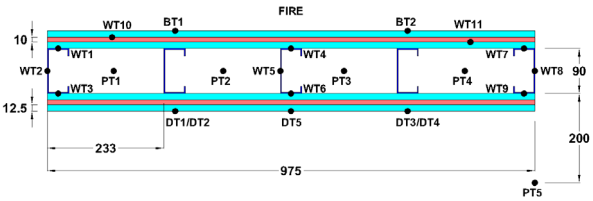

h) Thermocouples position in specimen 13.

i) Initial state of wall specimen 14.

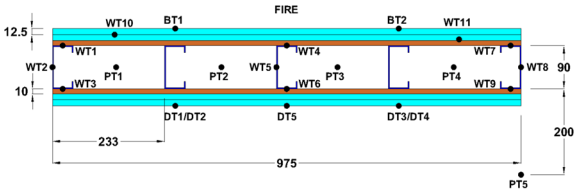

j) Thermocouples position in specimen 14.

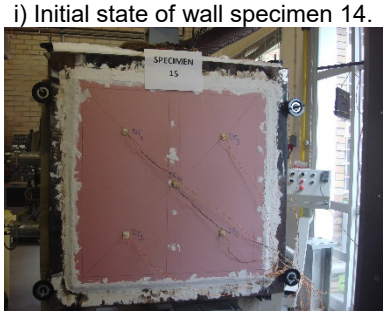

k) Initial state of wall specimen 15.

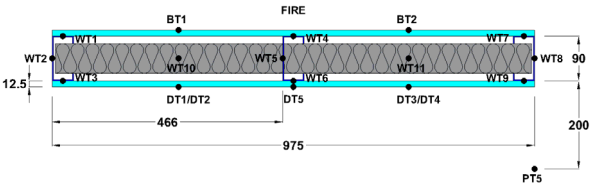

l) Thermocouples position in specimen 15.

Figure 3: Specimens and sensors for temperature measurement.

2.4 Fire tests results

The six LSF wall specimens were subjected to the ISO834 [19]. Different failure modes were achieved due to local and global buckling modes and identified as the ultimate limit state of the LSF frame. These failure modes are related with the thermal expansion of the steel frame. For the specimens 12, 13 and 14, the furnace temperature goes beyond the temperature curve of ISO 834 due to the heat release effect of the combustible materials (cork and OSB). The absence of the combustible materials in the other wall specimens explains the proximity of the furnace temperature with the ISO 834 curve, see Figure 4. The time history is presented with average values for some important regions on the left side, while the temperature field is presented on the right side for a specific time during the test.

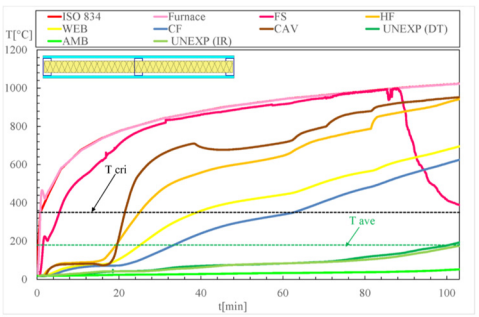

a) Average temperature results of test 10.

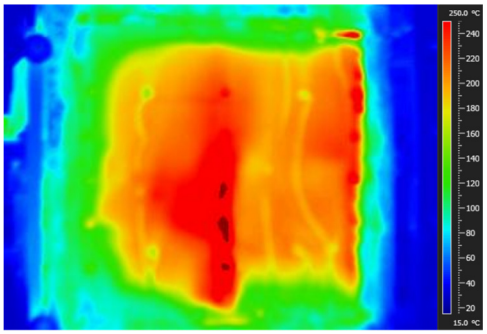

b) Temperature of IR camera at t=110 min.

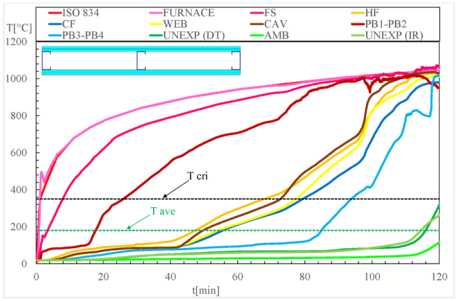

c) Average temperature results of test 11.

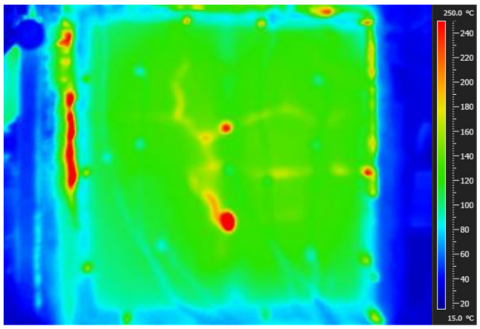

d) Temperature of IR camera at t=110 min.

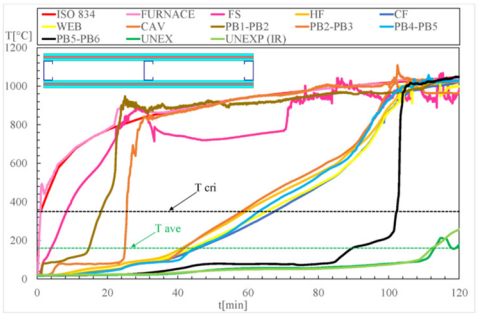

e) Average temperature results of test 12.

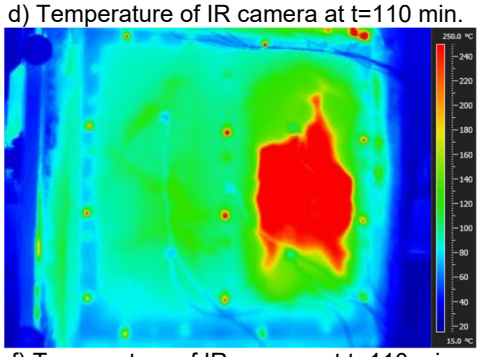

f) Temperature of IR camera at t=110 min.

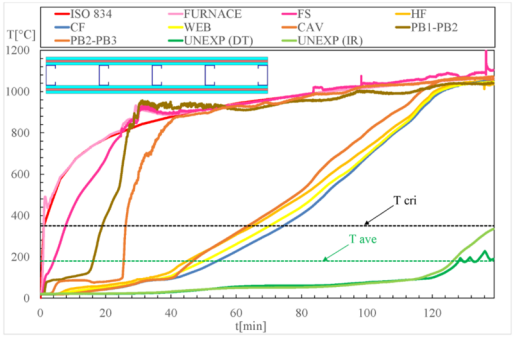

g) Average temperature results of test 13.

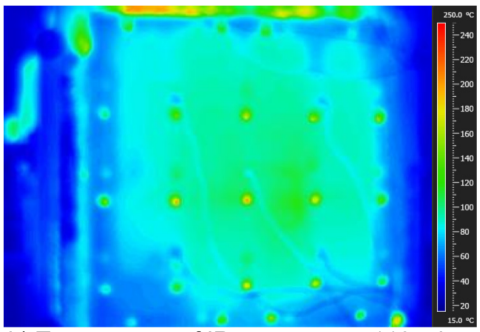

h) Temperature of IR camera at t=110 min.

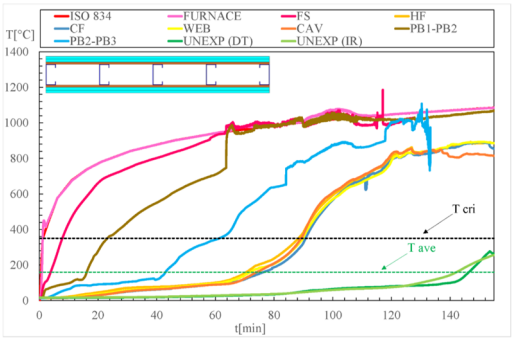

i) Average temperature results of test 14.

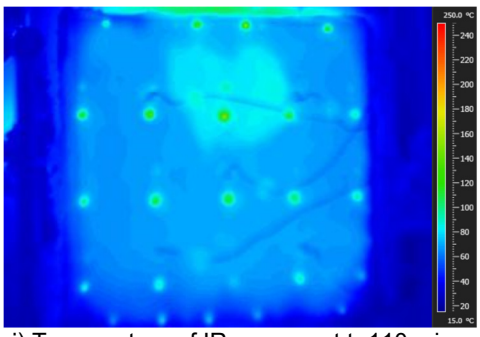

j) Temperature of IR camera at t=110 min.

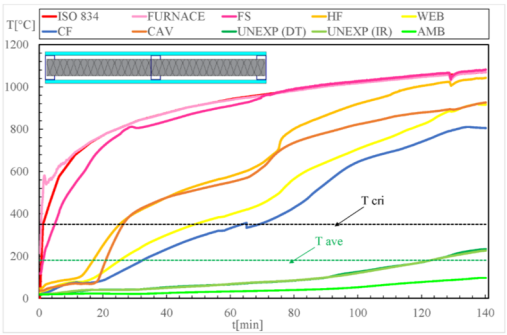

k) Average temperature results of test 15.

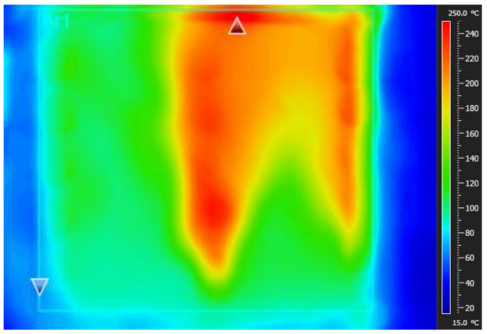

l) Temperature of IR camera at t=110 min.

Figure 4: Temperature results on specimens.

The maximum and average temperature of the unexposed side was determined using disc thermocouples UNEXP (DT), obtained from the individual measurements of DTi [1] and with a FLIR infrared thermal camera, located at 3m distance from the unexposed surface, UNEXP (IR). Special measurements were also defined for some specimens, such as: the average temperature of the cavity (CAV), obtained from the individual measurements of PTi; the room temperature (AMB) measured 200 mm away from the unexposed side of the LSF wall and the interface temperature (PBi-PBj) between the composite layered plates, obtained from the individual measurements of WTi. The results from IR camera and DT thermocouples and WT thermocouples for the measurement of the 3 steel stud components (hot, web, and cold flange) are presented in table 2.

Table 2: Results of the tested specimen used for fire rating [Fire resistance for insulation criteria (I) in completed minutes and Fire resistance for steel elements of class 4 (R)].

Specimen **ID**	DTmax (I) min	DTaver (I) min	IR aver (I) min	**HF=350 °C min**	**WEB=350 °C min**	**CF=350 °C (R) min**
10	79	95	99	25	39	62
11	114	115	113	68	79	77
12	112	113	112	59	65	67
13	128	127	125	65	70	74
14	145	146	142	88	90	91
15	95	115	115	25	48	63

3 NUMERICAL VALIDATION

3.1 Solution methods and models

In this investigation two different numerical solution methods were used to simulate the six fire tests of the non-loadbearing LSF wall. The first solution method uses thermal and fluid analysis for both parts, solid and fluid (ANSYS FLUENT). The flow analysis considers laminar fluid and is based on density variation. The fluid motion is induced by heat transfer and the solution is transient and nonlinear. The density-based solver solves the governing equations of continuity,

momentum and energy simultaneously. Pressure is obtained through the equation of state. Governing equations for additional scalars are solved afterward and sequentially (radiation). The integration time for each time step was 60 s, with the possibility to be reduced to 5 s. The convergence criterion was based on the residuals for each equation. The numerical model divides the cross section in finite cells. The domain variables (pressure, velocity, temperature) are calculated in each cell, at the same time. The grid for all the domains (solid and fluid) of specimen 11 is presented in Figure 5 (a, b), using the minimum size of the cell equal to 0.0005 m.

The second solution method uses ANSYS MULTIPHYSICS and considers only the thermal analysis for solids, assuming perfect contact between materials. The transient and nonlinear thermal analysis was selected, with full option solution method. The same time step was used with similar convergence criterion for the heat flow. Figure 5 (a,f) represents the mesh used for test 10 and 15. This solution method can be used with hybrid model for the temperature evolution in the cavity (average PTi value from the test results) as bulk temperature for the heat transfer due to convection and radiation, see Figure 5 (c,d,e). The density of the mesh used for ANSYS MULTIPHYSICS is smaller in comparison with the cells used in ANSYS FLUENT, nevertheless the thickness of the studs was divided into three finite elements as well. The mesh was defined based on a convergence test using calculation of the internal heat flow, with a minimum reference value of 1E-6 and a tolerance value of 0.001.

One side of the wall was submitted to fire and the other side is assumed to remain in contact with room temperature. The boundary conditions are defined in accordance to EN1991-1-2 [20], assuming heat transfer by radiation (emissivity of fire $\varepsilon_f = 1$) and convection (convection coefficient $\alpha_c = 25\ \mathrm{W/m^2K}$) in the exposed side and heat transfer by convection (convection coefficient $\alpha_c = 9\ \mathrm{W/m^2aK}$) in the unexposed side to include the radiation effect. The temperature in the exposed side follows the standard ISO834 [19]. The room temperature of the unexposed side was considered equal to the initial temperature, during all the simulation time.

In tests with a 3-layer composite panel 11, 12, 13 and 14, the same boundary conditions were assumed, but an extra boundary was applied on the node at the half height of the empty cavity that follows the effect of the fire curve coming from the experimental results of the cavity region of each specimen (CAV) – hybrid solution method. A convection inside the cavity was applied on all the lines that surround the cavity (convection coefficient $\alpha_c = 17.5\ \mathrm{W/m^2K}$), and radiation on the same lines that surround the cavity (emissivity of fire $\varepsilon_f = 1$), see Figure 5 (c, d, e).

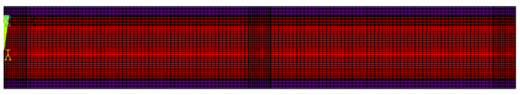

a) Solution method 2 for test specimen 10.

b) Solution method 1 for test specimen 11.

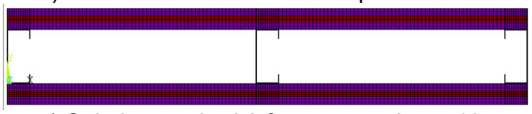

c) Solution method 2 for test specimen 12.

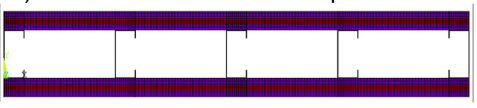

d) Solution method 2 for test specimen 13.

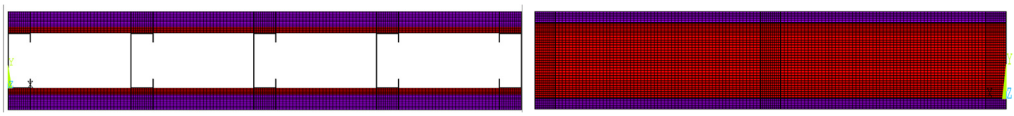

e) Solution method 2 for test specimen 14. f) Solution method 2) for test specimen 15.

Figure 5: Finite cells used in solution methods of the six test specimens.

The thermal properties of all the materials were considered temperature dependent. Figure 6 depicts all the major properties that were used to solve the energy equation. The steel properties were retrieved from EN1993-1-2 [21] and the gypsum properties were retrieved from the work developed by Mohamed Sultan [22]. The thermal properties of the cork and OSB assumed the same type of temperature dependence in accordance to the proposal of EN1995-1-2 [23], but small modifications were applied to the properties of cork, elimination of the specific heat peak value for the OSB and adjusting the values measured at room temperature by the hot disk method [24]. The thermal properties for the Rockwool were obtained from Steinar Lundberg [25], duly adapted to the corresponding material density. The emissivity of steel and cork was considered equal to 0.7, the emissivity of gypsum and OSB equal to 0.8. The properties of the super wool Blanket plus of density 128 Kg/m^3 were obtained from Morgan Thermal Ceramics [26], [27].

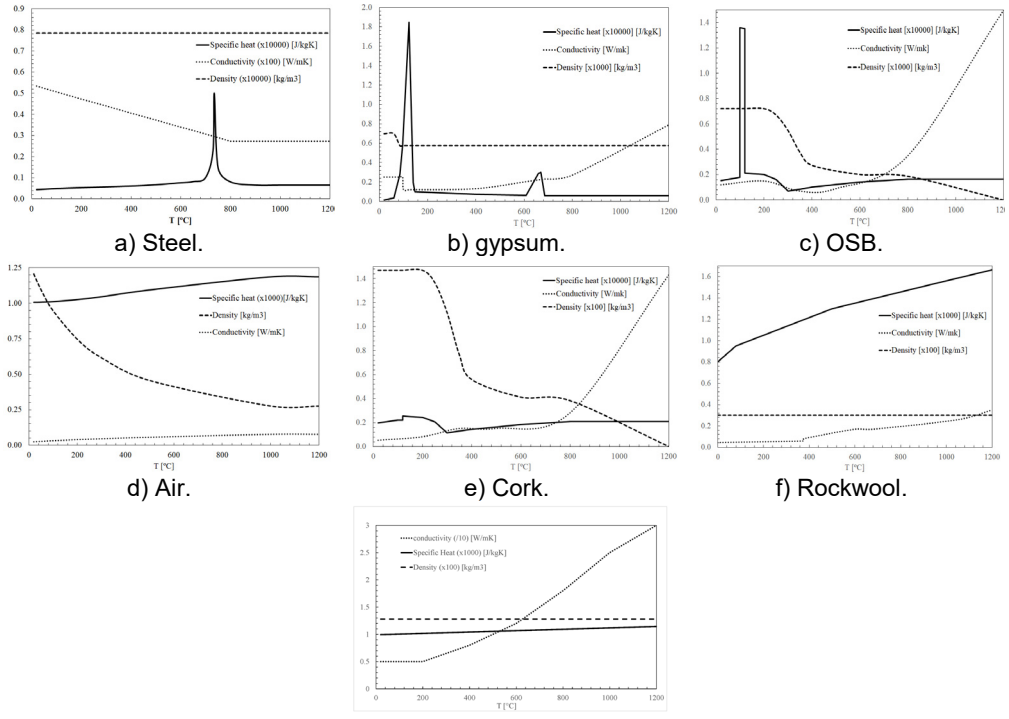

a) Steel. b) gypsum. c) OSB.

d) Air. e) Cork. f) Rockwool.

g) Superwool.

Figure 6: Thermal properties for all the materials involved in thermal simulation.

3.2 Results

The time history evolution for the temperature from each simulation is presented in Figure 7, collecting the nodal temperatures in the same regions where the thermocouples were located, in accordance to the tested specimen. On the numerical results of specimens 10 and 15 we noticed that the difference between hot flange (HF) and the cold flange (CF) was big due to the assumption of perfect contact between the insulation material in cavity (Rockwool, Superwool) and all other materials in contact with. This perfect contact is responsible for a temperature delay during the heating process. Rockwool and Superwool have a thermal conductivity higher than the one considered to simulate the fluid (air) in the cavity (specimen11). This justifies the higher conductivity resistance of the air in comparison to Rockwool or Superwool. The conductivity is the only mean of heat transfer in the solid filled cavity, while radiation and convection are also considered in the simulation of the fluid cavity and empty cavity. The specimens12, 13 and 14 present similar trends due to some similarity in the configuration of the LSF wall (absence of insulation material on the cavity and having a composite panel). The main difference between the experimental results and the numerical results can be justified by the localised effect of a crack, opening or the ignition of the combustible material.

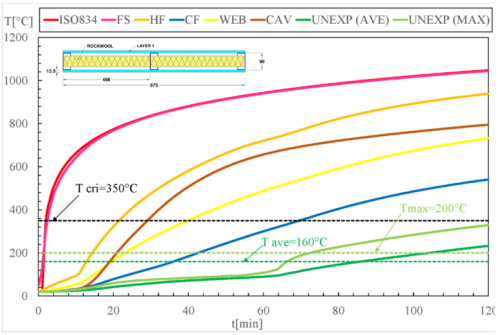

a) Results of simulation test specimen 10.

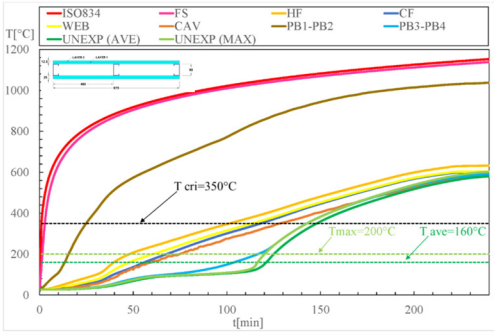

b) Results of simulation test specimen 11.

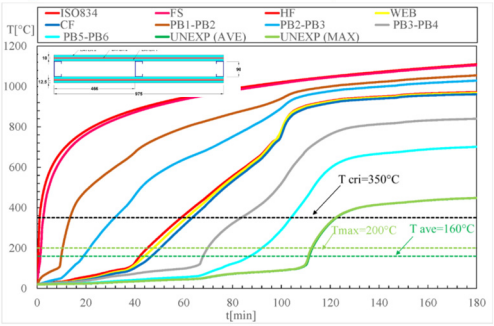

c) Results of simulation test specimen 12.

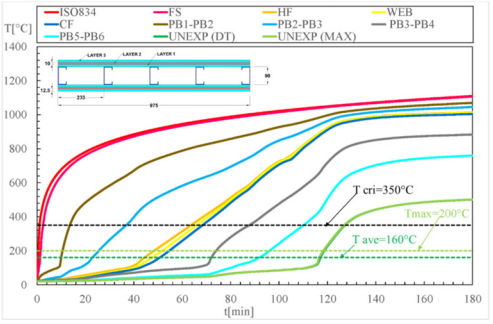

d) Results of simulation test specimen 13.

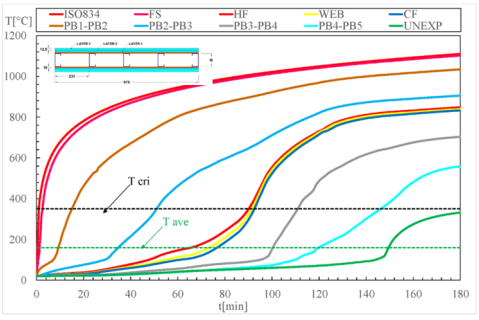

e) Results of simulation test specimen 14.

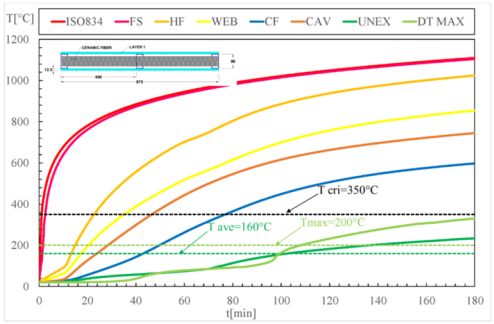

f) Results of simulation test specimen 15.

Figure 7: Time history for Temperature during the simulation of all the tests.

3.3 Comparison between the experimental and numerical results

The table 3 shows that the results of the fire tests agree well with the results from the numerical simulations. The difference between the results obtained for the fire resistance criteria are in between 0% and 13%. The comparison was made using the criteria (maximum temperature [T max] and average temperature [T ave]) applied to measure the insulation fire performance, using DT measurements from experiments and a representative number of nodal results from the unexposed side of the model, in completed minutes. The results agree well not only when using the criteria but also when comparing the time history of the temperature results.

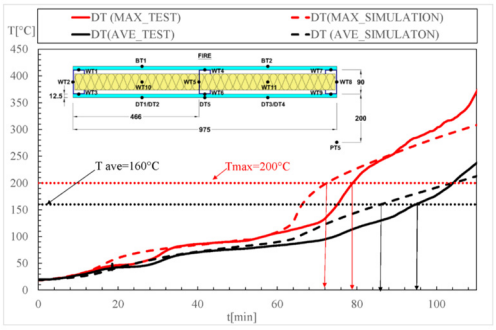

a) Time history comparison of specimen 10.

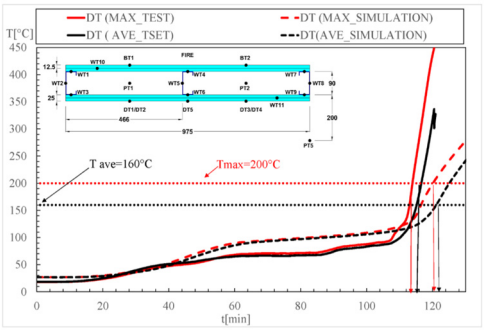

b) Time history comparison of specimen 11.

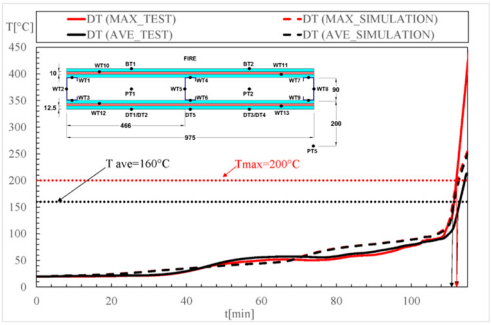

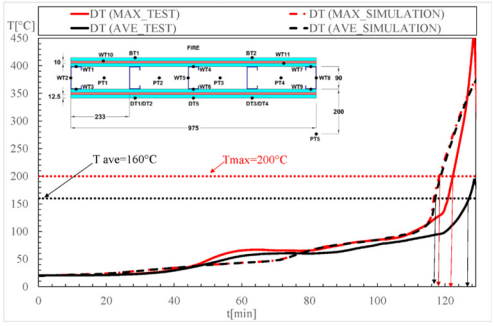

c) Time history comparison of specimen 12.

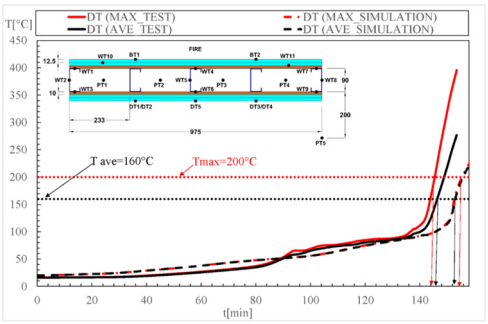

d) Time history comparison of specimen 13.

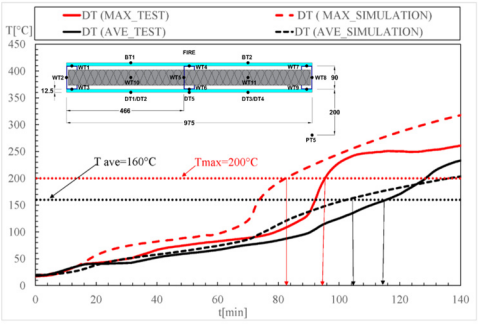

e) Time history comparison of specimen 14.

f) Time history comparison of specimen 15.

Figure 8: Time history comparison for the unexposed temperature (maximum and average) for each specimen.

Table 3: Comparison between numerical simulation and experimental results.

Specimen **ID**	DT max TEST min	DT max SIMULATION min	ERROR %	DT ave TEST **min**	DT ave SIMULATION **min**	**ERROR %**
10	79	72	8	95	86	10
11	114	121	7	115	122	8
12	112	112	0	113	112	0
13	128	118	3	127	117	7
14	145	151	4	146	153	4
15	95	83	12	115	105	8

4 CONCLUSIONS

This work has provided a summary of the detailed fire resistance study of six LSF non-load bearing based on both experimental and finite element studies. The different LSF walls were tasted in accordance with standards and the fire resistance was determined for insulation (I).

Different solution models were used to validate the experimental tests, using the finite volume method and finite element method. The hybrid solution method can be used to predict the fire resistance of partition walls, taking into consideration the heat transfer by convection and radiation inside the cavity. This solution method requires an extra temperature measurement for the evolution of the bulk temperature in the cavity and the selection of the appropriate heat flow coefficients. This measurement is of extreme importance to account for all the major events that may occur during tests (cracks and ignition of combustible materials).

The fire resistance of the LSF wall increases with the increment of the number of studs in the LSF and also with the thickness of the protection layers. It was clearly observed that the insulation of cavities brings relevant improvements to fire resistance

Specimen 14 presents higher fire resistance (I), mainly due to the higher stiffness of the OSB. Two gypsum layers (Specimen 11) performed better fire behaviour when compared to the single layer with cavity insulation (Specimens 10 and 15).

The Superwool seems to be the best insulation material to be applied in the cavity.

A good agreement was achieved between the numerical results and the results from the fire tests. The solution method 2, with hybrid model, is the best approximation (smaller relative error), because it is able to consider the failure of the gypsum plates, cracks and the ignition of the combustible materials (cork and OSB).

The results of the numerical validation and experimental tests provided the classification of fire resistance to the six partition walls (I 60 for wall specimens 10, 11, 12 and 15), (I120 for wall specimens 13 and 14).

5 FUTURE WORK

The 3D numerical validations of the tests are ongoing, and a new parametric analysis of the tests is also in development.

ACKNOWLEDGMENTS

Special thanks are due to the companies: Amorim Composites, FALPER / Fibroplac, F. Pereira building Materials and Normago.

REFERENCES

[1] CEN- European Committee for Standardization, EN 1363-1: Fire resistance tests Part 1 : General Requirements, CEN-Europ. Brussels, 2012.
[2] CEN- European Committee for Standardization, Ed., EN 1364-1: Fire resistance tests for non-loadbearing elements. Part 1: Walls, CEN-Europ. Brussels, 2015.
[3] A. Chajes, S. Britvec, and G. Winter. – “Effects of cold-straining on structural sheet steels”, Journal of the Structural Division, vol. 89, no. 2, pp. 1–32, 1963.
[4] Son, B. C., & Shoub, H. – “Fire Endurance Tests of Double Module Walls of Gypsum Board and Steel Studs” (Report). (National Bureau of Standards Washington, Ed.). Washington, D.C. 202234, 1973.
[5] K. J. Schwartz and T. T. Lie. – “Investigating the unexposed surface temperature criteria of standard ASTM e119”, Fire Technology, vol. 21, no. 3, 1985, pp. 169–180.
[6] Wanniarachchi, Somadasa. – “Flexural behaviour and design of cold-formed steel beams with rectangular hollow flanges”. PhD thesis, Queensland University of Technology, 2005.
[7] Gerlich, J. T. H. – “Design of Loadbearing Light Steel Frame Walls for Fire Resistance”, Fire Engineering Research Report, 1995, pp3-104, https://doi.org/ISSN 1173-5996.

[8] Alfawakhiri, Farid and Sultan, Mohamed A., "Fire Resistance of Loadbearing LSF Assemblies" 15th International Specialty Conference on Cold-Formed Steel Structures. St. Louis, MO, U.S.A. http://scholarsmine.mst.edu/isccss/15iccfss/15iccfss-session9/1, October 2000.

[9] Ghazi Wakili, K., & Hugi, E. – "Four types of gypsum plaster boards and their thermophysical properties under fire condition". Journal of Fire Sciences, 27(1), 2009, pp 27–43. https://doi.org/10.1177/0734904108094514.

[10] A.Y. Nassif, I. Yoshitake, A. Allam. – "Full-scale fire testing and numerical modelling of the transient thermo-mechanical behaviour of steel-stud gypsum board partition walls", journal of Construction and Building Materials. 59, 2014, pp 51–61, http://dx.doi.org/10.1016/j.conbuildmat.2014.02.027.

[11] Jonathan Vallée. - "Reliability of fire barriers Lund University", Msc thesis, Faculty of Engineering Department, 2016.

[12] Piloto, P. A. G., Khetata, M. S., & Gavilán. A. B. R. – "Fire performance of non-loadbearing light steel framing walls - numerical simulation". In 7th international conference mechanics and materials in design, 2017, pp. 1603–1610. Albufeira, Portugal: INEGI/FEUP.

[13] Khetata, M., Fernandes, L., Marinho, C., Piloto, P., Gavilán, A., & Razuk, H. – "Fire resistance of non-loadbearing light steel framing walls: numerical validation". In XI Portuguese Congress on Steel and Composite Construction – CMM 2017, pp. 853–862. Coimbra, Portugal: Portuguese Association for Steel and Composite Construction.

[14] Piloto, P. A. G., Khetata, M. S., & Gavilán, A. B. R. – "Fire Performance of Non-Loadbearing Light Steel Framing Walls-Numerical and simple calculation methods", MATTER: International Journal of Science and Technology, 3(3),2017, pp13–23. https://doi.org/https://dx.doi.org/10.20319/mijst.2017.33.1323 .

[15] Piloto, P. A. G. – "Fire resistance of cold-formed steel walls with composite panels: Results from insulation rating (I) and loadbearing prediction rating (R)", Metálica International, (7), 2018, pp12–17.

[16] Piloto, P. A. G., Khetata, M. S., & Gavilán, A. B. R. – "Loadbearing Capacity of LSF Walls under Fire Exposure", MATTER: International Journal of Science and Technology,2018 ISSN pp 2454-5880, Volume 4, Issue 3, pp. 104-124, DOI- https://dx.doi.org/10.20319/mijst.2018.43.104124.

[17] Paulo Piloto, Mohamed Khetata, Ana Gavilán. – "Fire Resistance of non-loadbearing LSF walls", TEST&E 2019, ISEP, Porto, 2019, book of abstracts, pp. 40-41.

[18] Yomal Dias, Pologanathan Keerthan, Mahen Mahendran. – "Fire performance of steel and plasterboard sheathed non-load bearing LSF walls", Fire Safety Journal 103, 2019, pp 1–18, https://doi.org/10.1016/j.firesaf.2018.11.005.

[19] International Organization for Standardization. ISO834-1: Fire-resistance tests - Elements of building construction - Part 1: General requirements.1999.

[20] CEN- European Committee for Standardization, EN1991-1-2 - Eurocode 1: Actions on Structures - Part 1-2: General Actions - "Actions on Structures Exposed to Fire." Brussels: CEN, 2002, p: 59.

[21] CEN- European Committee for Standardization. EN1993-1-2: European Standard Eurocode 3: "Design of steel structures" - Part 1-2: General rules - Structural fire design. (CEN-European Committee for Standardization, Ed.) (CEN-Europ). Brussels: CEN- European Committee for Standardization, 2005.

[22] Sultan, M. A. “A model for predicting heat transfer through non insulated unloaded steel-stud gypsum board wall assemblies exposed to fire”. Fire Technology, 32(3), pp 239–259, 1996, https://doi.org/10.1007/BF01040217.
[23] CEN- European Committee for Standardization, 2004). EN 1995-1-2 : Eurocode 5 – “Design of timber structures”.Part 1-2 : General – Structural fire design. (CEN- European Committee for Standardization, Ed.), CEN- European Committee for Standardization (CEN-Europ). CEN- European Committee for Standardization.
[24] International Organization for Standardization. (2015). 22007-2: “Plastics — Determination of thermal conductivity and thermal diffusivity — Part 2: Transient plane heat source (hot disc) method”. (International Organization for Standardization, Ed.). International Organization for Standardization.
[25] Lundberg, S. “Material Aspects of Fire Design” – TALAT, 1994, Lectures 2502.
[26] Morgan advanced materials, “Thermal Ceramics-Data sheet Superwool blanket”, pp 1-3, 2016.
[27] Morgan advanced materials, “Thermal Ceramics, Superwool Plus Insulating fibre”, section1, 1.6, pp 29-34, 2016.


CIN
PROTECTIVE COATINGS
CILASCI
5